Available online at www.sciencedirect.com
ScienceDirect
International Journal of Thermal Sciences 46 (2007) 1251–1258
International Journal of Thermal Sciences
www.elsevier.com/locate/ijts

Radiation and mass transfer effects on two-dimensional flow past an impulsively started infinite vertical plate

V. Ramachandra Prasad [a,*], N. Bhaskar Reddy [a], R. Muthucumaraswamy [b]

[a] *Department of Mathematics, Sri Venkateswara University, Tirupati – 517502, India*
[b] *Department of Information Technology, Sri Venkateswara College of Engineering, Sriperumbudur – 602105, India*

Received 13 March 2006; received in revised form 27 December 2006; accepted 2 January 2007
Available online 20 February 2007

Abstract

The interaction of free convection with thermal radiation of a viscous incompressible unsteady flow past an impulsively started vertical plate with heat and mass transfer is analyzed. The fluid is gray, absorbing-emitting but non-scattering medium and the Rosseland approximation is used to describe the radiative flux in the energy equation. The dimensionless governing equations are solved using an implicit finite-difference method of Crank–Nicolson type. Numerical results for the velocity, the temperature, the concentration, the local and average skin-friction, the Nusselt number and Sherwood number are shown graphically. It is observed that, when the radiation parameter increases, the velocity and temperature decrease in the boundary layer. The local and average skin-friction increases with the increase in radiation parameter. For increasing values of radiation parameter the local as well as average Nusselt number increases.

Keywords: Heat transfer; Radiation; Finite difference method

1. Introduction

Stokes [1] first presented an exact solution to the Navier–Stokes equation, which is the flow of a viscous incompressible fluid past an impulsively started infinite horizontal plate in its own plane. It is often called Rayleigh problem in the literature. Such a flow past an impulsively started semi-infinite horizontal plate was first presented by Stewartson [2]. Hall [3] obtained the numerical solution for the problem of boundary layer over an impulsively started semi-infinite horizontal plate. However, in Hall's analysis only unsteady velocity field was studied as buoyancy effects were considered to be negligible. Soundalgekar [4] presented an exact solution to the flow of a viscous fluid past an impulsively started infinite with constant heat flux and chemical reaction. The solution was derived by the Laplace transform technique and the effects of heating or cooling of the plate on the flow field were discussed through Grashof number. Raptis [5] studied flow past an impulsively started infinite vertical plate in a porous medium by a finite difference method.

Many transport processes exist in nature and in industrial applications in which the simultaneous heat and mass transfer occur as a result of combined buoyancy effects of thermal diffusion and diffusion of chemical species. A few representative fields of interest in which combined heat and mass transfer plays an important role are designing of chemical processing equipment, formation and dispersion of fog, distribution of temperature and moisture over agricultural fields and groves of fruit trees, crop damage due to freezing, and environmental pollution. In this context Soundalgekar [6] extended his own problem of [4] to mass transfer effects. Das et al. [7] considered the mass transfer effects on the flow past an impulsively started infinite isothermal vertical plate with constant mass flux and chemical reaction. Muthucumaraswamy and Ganesan [8] considered the problem of unsteady flow past an impulsively started isothermal vertical plate with mass transfer by an implicit finite difference method. Muthucumaraswamy and Ganesan [9,10] solved the problem of unsteady flow past an impulsively started vertical plate with uniform heat and mass flux and variable temperature and mass flux respectively.

* Corresponding author.
E-mail address: rcpmaths@yahoo.com (V.R. Prasad).

1290-0729/$ – see front matter
doi:10.1016/j.ijthermalsci.2007.01.004

Nomenclature

C'	concentration
C	dimensionless concentration
D	mass diffusion coefficient
g	acceleration due to gravity
Gm	solutal Grashof number
Gr	thermal Grashof number
L	reference length
N	conduction–radiation parameter
Nu_x	local Nusselt number
$\overline{Nu}_L$	average Nusselt number
Nu_X	dimensionless local Nusselt number
$\overline{Nu}$	dimensionless average Nusselt number
Pr	Prandtl number
q_r	radiative heat flux
Sc	Schmidt number
Sh_x	local Sherwood number
$\overline{Sh}_L$	average Sherwood number
Sh_X	dimensionless local Sherwood number
$\overline{Sh}$	dimensionless average Sherwood number
T'	temperature
T	dimensionless temperature
t'	time
t	dimensionless time
u_0	velocity of the plate
$u,\ v$	velocity components in $x,\ y$-directions respectively
x	spatial coordinate along the plate
X	dimensionless spatial coordinate along the plate
y	spatial coordinate normal to the plate
Y	dimensionless spatial coordinate normal to the plate

Greek symbols

α	thermal diffusivity
β	volumetric coefficient of thermal expansion
β^*	volumetric coefficient of expansion with concentration
μ	dynamic viscosity
ν	kinematic viscosity
ρ	density
τ'	local skin-friction
$\overline{\tau}_L$	average skin-friction
τ_X	dimensionless local skin-friction
$\overline{\tau}$	dimensionless average skin-friction

Subscripts

w	conditions on the wall
∞	free stream conditions

In the context of space technology and in processes involving high temperatures the effects of radiation are of vital importance. Recent developments in hypersonic flights, missile reentry, rocket combustion chambers, power plants for inter planetary flight and gas cooled nuclear reactors, have focused attention on thermal radiation as a mode of energy transfer, and emphasize the need for improved understanding of radiative transfer in these processes. The interaction of radiation with laminar free convection heat transfer from a vertical plate was investigated by Cess [11] for an absorbing, emitting fluid in the optically thick region, using the singular perturbation technique. Arpaci [12] considered a similar problem in both the optically thin and optically thick regions and used the approximate integral technique and first-order profiles to solve the energy equation. Cheng and Ozisik [13] considered a related problem for an absorbing, emitting and isotropically scattering fluid, and treated the radiation part of the problem exactly with the normal-mode expansion technique. Raptis [14] has analyzed the thermal radiation and free convection flow through a porous medium by using perturbation technique. Hossain and Takhar [15] studied the radiation effects on mixed convection along a vertical plate with uniform surface temperature using Keller Box finite difference method. In all these papers the flow is considered to be steady. Mansour [16] studied the radiative and free convections effects on the oscillatory flow past a vertical plate. Raptis and Perdikis [17] studied the effects of thermal radiation and free convective flow past moving plate. Das et al. [18] have analyzed the radiation effects on flow past an impulsively started infinite isothermal vertical plate. The governing equations were solved by the Laplace transform technique. Chamkha et al. [19] have studied the radiation effects on free convection flow past a semi-infinite vertical plate with mass transfer.

The aim of the present paper is to study unsteady, laminar, simultaneous free convective heat and mass transfer flow along an impulsively started plate in the presence of thermal radiation effects. The solution of the problem is obtained by using an implicit finite difference method of Crank–Nicolson type.

2. Mathematical analysis

Consider a two-dimensional, transient, laminar, natural convection flow of an incompressible viscous radiating fluid past an impulsively started vertical plate. It is assumed that the concentration C' of the diffusing species in the binary mixture is very less in comparison to the other chemical species, which are present. This leads to the assumption that the Soret and Dufour effects are negligible. It is also assumed that the effect of viscous dissipation is negligible in the energy equation. The x-axis is taken along the plate in the upward direction and the y-axis is taken normal to it. At $t' > 0$, the plate starts impulsively in the vertical direction with constant velocity u_0 against the gravitational field. Also, the temperature of the plate and the concentration level near the plate are raised, and are maintained constantly thereafter. Then under the above assumptions, the governing boundary layer equations of mass, momentum, energy and species concentration for free convective flows with Boussinesq's approximation are as follows.

$$\frac{\partial u}{\partial x}+\frac{\partial v}{\partial y}=0 \tag{1}$$

$$\frac{\partial u}{\partial t'}+u\frac{\partial u}{\partial x}+v\frac{\partial u}{\partial y} = g\beta(T'-T'_\infty)+g\beta^*(C'-C'_\infty)+\nu\frac{\partial^2 u}{\partial y^2} \tag{2}$$

$$\frac{\partial T'}{\partial t'}+u\frac{\partial T'}{\partial x}+v\frac{\partial T'}{\partial y}=\alpha\frac{\partial^2 T'}{\partial y^2}-\frac{1}{\rho c_p}\frac{\partial q_r}{\partial y} \tag{3}$$

$$\frac{\partial C'}{\partial t'}+u\frac{\partial C'}{\partial x}+v\frac{\partial C'}{\partial y}=D\frac{\partial^2 C'}{\partial y^2} \tag{4}$$

The initial and boundary conditions are

$$\left.\begin{array}{l} t'\leqslant 0\text{: } u=0,\quad v=0,\quad T'=T'_\infty,\quad C'=C'_\infty \\ t'>0\text{: } u=u_0,\quad v=0,\quad T'=T'_w,\quad C'=C'_w \\ \quad \text{at } y=0 \\ u=0,\quad T'=T'_\infty,\quad C'=C'_\infty \quad \text{at } x=0 \\ u\to 0,\quad T'\to T'_\infty,\quad C'\to C'_\infty \quad \text{as } y\to\infty \end{array}\right\} \tag{5}$$

We now assume Rosseland approximation (Brewster [20]), which leads to the radiative heat flux q_r is given by

$$q_r=-\frac{4\sigma_s}{3k_e}\frac{\partial T'^4}{\partial y} \tag{6}$$

where σ_s is the Stefan–Boltzmann constant and k_e is the mean absorption coefficient, respectively. It should be noted that by using the Rosseland approximation we limit our analysis to optically thick fluids. If temperature differences within the flow are sufficiently small, then Eq. (6) can be linearized by expanding T'^4 into the Taylor series about T'_∞, which after neglecting higher order terms takes the form:

$$T'^4\cong 4T'^3_\infty T'-3T'^4_\infty \tag{7}$$

In view of Eqs. (6) and (7), Eq. (3) reduces to

$$\frac{\partial T'}{\partial t'}+u\frac{\partial T'}{\partial x}+v\frac{\partial T'}{\partial y}=\alpha\frac{\partial^2 T'}{\partial y^2}+\frac{16\sigma_s T'^3_\infty}{3k_e\rho c_p}\frac{\partial^2 T'}{\partial y^2} \tag{8}$$

Local as well as average values of skin-friction, Nusselt number and Sherwood number [8] are as follows:

$$\tau'=-\mu\left(\frac{\partial u}{\partial y}\right)_{y=0} \tag{9}$$

$$\bar{\tau}_L=\frac{-1}{L}\int_0^L \mu\left(\frac{\partial u}{\partial y}\right)_{y=0}\mathrm{d}x \tag{10}$$

$$Nu_x=\frac{-x(\partial T'/\partial y)_{y=0}}{T'_w-T'_\infty} \tag{11}$$

$$\overline{Nu}_L=-\int_0^L\left[\left(\frac{\partial T'}{\partial y}\right)_{y=0}\Big/(T'_w-T'_\infty)\right]\mathrm{d}x \tag{12}$$

$$Sh_x=\frac{-x(\partial C'/\partial y)_{y=0}}{C'_w-C'_\infty} \tag{13}$$

$$\overline{Sh}_L=-\int_0^L\left[\left(\frac{\partial C'}{\partial y}\right)_{y=0}\Big/(C'_w-C'_\infty)\right]\mathrm{d}x \tag{14}$$

On introducing the following non-dimensional quantities

$$\left.\begin{array}{ll} X=\frac{xu_0}{\nu}, & Y=\frac{yu_0}{\nu}, \quad t=\frac{t'u_0^2}{\nu} \\ U=\frac{u}{u_0}, & V=\frac{v}{u_0} \\ Gr=\frac{\nu g\beta(T'_w-T'_\infty)}{u_0^3}, & Gm=\frac{\nu g\beta^*(C'_w-C'_\infty)}{u_0^3} \\ N=\frac{kk_e}{4\sigma_s T'^3_\infty}, & T=\frac{T'-T'_\infty}{T'_w-T'_\infty}, \quad C=\frac{C'-C'_\infty}{C'_w-C'_\infty} \\ Pr=\frac{\nu}{\alpha}, & Sc=\frac{\nu}{D} \end{array}\right\} \tag{15}$$

Eqs. (1), (2), (8) and (4) are reduced to the following non-dimensional form

$$\frac{\partial U}{\partial X}+\frac{\partial V}{\partial Y}=0 \tag{16}$$

$$\frac{\partial U}{\partial t}+U\frac{\partial U}{\partial X}+V\frac{\partial U}{\partial Y}=Gr\,T+Gm\,C+\frac{\partial^2 U}{\partial Y^2} \tag{17}$$

$$\frac{\partial T}{\partial t}+U\frac{\partial T}{\partial X}+V\frac{\partial T}{\partial Y}=\frac{1}{Pr}\left(1+\frac{4}{3N}\right)\frac{\partial^2 T}{\partial Y^2} \tag{18}$$

$$\frac{\partial C}{\partial t}+U\frac{\partial C}{\partial X}+V\frac{\partial C}{\partial Y}=\frac{1}{Sc}\frac{\partial^2 C}{\partial Y^2} \tag{19}$$

The corresponding initial and boundary conditions are

$$\left.\begin{array}{l} t\leqslant 0\text{: } U=0,\quad V=0,\quad T=0,\quad C=0 \\ t>0\text{: } U=1,\quad V=0,\quad T=1,\quad C=1 \quad \text{at } Y=0 \\ U=0,\quad T=0,\quad C=0 \quad \text{at } X=0 \\ U\to 0,\quad T\to 0,\quad C\to 0 \quad \text{as } Y\to\infty \end{array}\right\} \tag{20}$$

using the non-dimensional quantities specified in (15), local as well as average values of skin-friction, Nusselt number and Sherwood number are as follows:

$$\tau_X=\frac{\tau'}{\rho u_0^2}=-\left(\frac{\partial U}{\partial Y}\right)_{Y=0} \tag{21}$$

$$\bar{\tau}=-\int_0^1\left(\frac{\partial U}{\partial Y}\right)_{Y=0}\mathrm{d}X \tag{22}$$

$$Nu_X=-X\left(\frac{\partial T}{\partial Y}\right)_{Y=0} \tag{23}$$

$$\overline{Nu}=-\int_0^1\left(\frac{\partial T}{\partial Y}\right)_{Y=0}\mathrm{d}X \tag{24}$$

$$Sh_X=-X\left(\frac{\partial C}{\partial Y}\right)_{Y=0} \tag{25}$$

$$\overline{Sh}=-\int_0^1\left(\frac{\partial C}{\partial Y}\right)_{Y=0}\mathrm{d}X \tag{26}$$

3. Numerical technique

In order to solve these unsteady, non-linear coupled equations (16) to (19) under the conditions (20), an implicit finite difference scheme of Crank–Nicolson type has been employed. The finite difference equations corresponding to Eqs. (16)–(19) are as follows:

$$\begin{aligned}&\big[U_{i,j}^{n+1}-U_{i-1,j}^{n+1}+U_{i,j}^{n}-U_{i-1,j}^{n}+U_{i,j-1}^{n+1}-U_{i-1,j-1}^{n+1}\\&\quad+U_{i,j-1}^{n}-U_{i-1,j-1}^{n}\big]/(4\Delta X)\\&\quad+\big[V_{i,j}^{n+1}-V_{i,j-1}^{n+1}+V_{i,j}^{n}-V_{i,j-1}^{n}\big]/(2\Delta Y)=0\end{aligned}\tag{27}$$

$$\begin{aligned}&\big[U_{i,j}^{n+1}-U_{i,j}^{n}\big]/\Delta t+U_{i,j}^{n}\big[U_{i,j}^{n+1}-U_{i-1,j}^{n+1}\\&\quad+U_{i,j}^{n}-U_{i-1,j}^{n}\big]/(2\Delta X)\\&\quad+V_{i,j}^{n}\big[U_{i,j+1}^{n+1}-U_{i,j-1}^{n+1}+U_{i,j+1}^{n}-U_{i,j-1}^{n}\big]/(4\Delta Y)\\&=Gr\big[T_{i,j}^{n+1}+T_{i,j}^{n}\big]/2+Gm\big[C_{i,j}^{n+1}+C_{i,j}^{n}\big]/2\\&\quad+\big[U_{i,j-1}^{n+1}-2U_{i,j}^{n+1}+U_{i,j+1}^{n+1}+U_{i,j+1}^{n+1}\\&\quad-2U_{i,j}^{n}+U_{i,j+1}^{n}\big]/(2(\Delta Y)^2)\end{aligned}\tag{28}$$

$$\begin{aligned}&\big[T_{i,j}^{n+1}-T_{i,j}^{n}\big]/\Delta t+U_{i,j}^{n}\big[T_{i,j}^{n+1}-T_{i-1,j}^{n+1}\\&\quad+T_{i,j}^{n}-T_{i-1,j}^{n}\big]/(2\Delta X)\\&\quad+V_{i,j}^{n}\big[T_{i,j}-T_{i,j-1}^{n+1}+T_{i,j+1}^{n}-T_{i,j-1}^{n}\big]/(4\Delta Y)\\&=\frac{1}{Pr}\left(1+\frac{4}{3N}\right)\big[T_{i,j-1}^{n+1}-2T_{i,j}^{n+1}+T_{i,j+1}^{n+1}+T_{i,j-1}^{n}\\&\quad-2T_{i,j}^{n}+T_{i,j+1}^{n}\big]/(2(\Delta Y)^2)\end{aligned}\tag{29}$$

$$\begin{aligned}&\big[C_{i,j}^{n+1}-C_{i,j}^{n}\big]/\Delta t+U_{i,j}^{n}\big[C_{i,j}^{n+1}-C_{i-1,j}^{n+1}\\&\quad+C_{i,j}^{n}-C_{i-1,j}^{n}\big]/(2\Delta X)\\&\quad+V_{i,j}^{n}\big[C_{i,j+1}^{n+1}-C_{i,j-1}^{n+1}+C_{i,j+1}^{n}-C_{i,j-1}^{n}\big]/(4\Delta Y)\\&=\frac{1}{Sc}\big[C_{i,j-1}^{n+1}-2C_{i,j}^{n+1}+C_{i,j+1}^{n+1}+C_{i,j-1}^{n}\\&\quad-2C_{i,j}^{n}+C_{i,j+1}^{n}\big]/(2(\Delta Y)^2)\end{aligned}\tag{30}$$

The region of integration is considered as a rectangle with sides $X_{\max}$ (= 1) and $Y_{\max}$ (= 14), where $Y_{\max}$ corresponds to $Y=\infty$ which lies very well outside the momentum, energy and concentration boundary layers. The maximum of Y was chosen as 14 after some preliminary investigations, so that the last two of the boundary conditions (20) are satisfied. Here, the subscript i – designates the grid point along the X-direction, j – along the Y-direction and the superscript n along the t-direction. An appropriate mesh size considered for the calculation is $\Delta X=0.05$, $\Delta Y=0.25$, and time step $\Delta t=0.01$. During any one-time step, coefficients $U_{i,j}^{n}$ and $V_{i,j}^{n}$ appearing in the difference equations are treated as constants. The values of U, V, T and C are known at all grid points at $t=0$ from the initial conditions. The computations of U, V, T and C at time level $(n+1)$ using the known values at previous time level (n) are calculated as follows: The finite difference equation (30) at every internal nodal point on a particular i-level constitute a tri-diagonal system of equations. Such a system of equations is solved by Thomas algorithm as described in Carnahan et al. [21]. Thus, the values of C are found at every nodal point on a particular i at $(n+1)$th time level. Similarly the values of T are calculated from Eq. (29). Using the values of C and T at $(n+1)$th time level in Eq. (28), the values of U at $(n+1)$th time level are found in a similar manner. Thus the values of C, T and U are known on a particular i-level. The values of V are calculated explicitly using Eq. (27) at every nodal point on a particular i-level at $(n+1)$th time level. This process is repeated for various i-levels. Thus the values of C, T, U and V are known at all grid points in the rectangular region at $(n+1)$th time level.

Computations are carried out till the steady-state is reached. The steady-state solution is assumed to have been reached, when the absolute difference between values of U as well as temperature T and concentration C at two consecutive time steps are less than 10^{-5} at all grid points. The derivatives involved in Eqs. (21)–(26) are evaluated using five-point approximation formula and integrals are evaluated using Newton–Cotes closed integration formula.

4. Stability analysis

The stability criterion of the finite difference scheme for constant mesh sizes are found using von Neumann techniques as explained in Carnahan et al. [21]. The general term of the Fourier expansion for U, T and C at a time arbitrarily called $t=0$ are assumed to be of the form $e^{i\alpha X}e^{i\beta Y}$ (here $i=\sqrt{-1}$). At a later time t, these terms will become

$$\left.\begin{aligned}U&=F(t)e^{i\alpha X}e^{i\beta Y}\\T&=G(t)e^{i\alpha X}e^{i\beta Y}\\C&=H(t)e^{i\alpha X}e^{i\beta Y}\end{aligned}\right\}\tag{31}$$

Substituting (31) in Eqs. (28)–(30); under the assumption that the coefficients U and V are constants over any one time step and denoting the values after one time step by F', G' and H', one may get after simplification.

$$\begin{aligned}&\frac{F'-F}{\Delta t}+\frac{U(F'+F)(1-e^{-i\alpha\Delta X})}{2\Delta X}\\&\quad+\frac{V(F'+F)i\sin(\beta\Delta Y)}{2\Delta Y}\\&=\frac{(G'+G)}{2}Gr+\frac{(H+H')}{2}Gm\\&\quad+\frac{(F'+F)(\cos\beta\Delta Y-1)}{(\Delta Y)^2}\end{aligned}\tag{32}$$

$$\begin{aligned}&\frac{G'-G}{\Delta t}+\frac{U(G'+G)(1-e^{-i\alpha\Delta X})}{2\Delta X}\\&\quad+\frac{V(G'+G)i\sin(\beta\Delta Y)}{2\Delta Y}\\&=\frac{(G'+G)(\cos\beta\Delta Y-1)}{Pr(\Delta Y)^2}\end{aligned}\tag{33}$$

$$\begin{aligned}&\frac{H'-H}{\Delta t}+\frac{U(H'+H)(1-e^{-i\alpha\Delta X})}{2\Delta X}\\&\quad+\frac{V(H'+H)i\sin(\beta\Delta Y)}{2\Delta Y}\\&=\frac{(H'+H)(\cos\beta\Delta Y-1)}{Sc(\Delta Y)^2}\end{aligned}\tag{34}$$

Eqs. (32)–(34) can be written as

$$\begin{aligned}(1+A)F'&=(1-A)F+\frac{Gr(G'+G)}{2}\Delta t\\&\quad+\frac{Gm(H'+H)}{2}\Delta t\end{aligned}\tag{35}$$

$$(1+B)G' = (1-B)G \tag{36}$$

$$(1+E)H' = (1-E)H \tag{37}$$

where

$$A = \frac{U}{2}\frac{\Delta t}{\Delta X}\left(1-\mathrm{e}^{-\mathrm{i}\alpha\Delta X}\right) + \frac{V}{2}\frac{\Delta t}{\Delta Y}\mathrm{i}\sin(\beta\Delta Y) - (\mathrm{Cos}\,\beta\Delta Y - 1)\frac{\Delta t}{(\Delta Y)^2}$$

$$B = \frac{U}{2}\frac{\Delta t}{\Delta X}\left(1-\mathrm{e}^{-\mathrm{i}\alpha\Delta X}\right) + \frac{V}{2}\frac{\Delta t}{\Delta Y}\mathrm{i}\sin(\beta\Delta Y) - \frac{\mathrm{Cos}\,\beta\Delta Y - 1}{Pr}\frac{\Delta t}{(\Delta Y)^2}$$

$$E = \frac{U}{2}\frac{\Delta t}{\Delta X}\left(1-\mathrm{e}^{-\mathrm{i}\alpha\Delta X}\right) + \frac{V}{2}\frac{\Delta t}{\Delta Y}\mathrm{i}\sin(\beta\Delta Y) - \frac{\mathrm{Cos}\,\beta\Delta Y - 1}{Sc}\frac{\Delta t}{(\Delta Y)^2}$$

After eliminating G' and H' in Eq. (35) using Eqs. (36) and (37), the resultant equation and equations can be written as follows:

$$\begin{bmatrix} F' \\ G' \\ H' \end{bmatrix} = \begin{bmatrix} \frac{1-A}{1+A} & D_1 & D_2 \\ 0 & \frac{1-B}{1+B} & 0 \\ 0 & 0 & \frac{1-E}{1+E} \end{bmatrix} \begin{bmatrix} F \\ G \\ H \end{bmatrix} \tag{38}$$

where

$$D_1 = \frac{\Delta t Gr}{(1+A)(1+B)} \quad \text{and} \quad D_2 = \frac{\Delta t Gm}{(1+A)(1+E)}.$$

Now, for stability the modulus of each eigen values of the amplification matrix must not exceed unity. The eigen values of the amplification matrix are $(1-A)/(1+A)$, $(1-B)/(1+B)$ and $(1-E)/(1+E)$. Assume that U is everywhere non-negative and V is everywhere non-positive, we get that

$$A = 2a\sin^2(\alpha\Delta X/2) + 2c\sin^2(\beta\Delta Y/2) + \mathrm{i}(a\sin\alpha\Delta X - b\sin\beta\Delta Y)$$

where

$$a = \frac{U\Delta t}{2\Delta X}, \quad b = \frac{|V|\Delta t}{2\Delta Y} \quad \text{and} \quad c = \frac{\Delta t}{(\Delta Y)^2}$$

Since the real part of A is greater than or equal to zero $|(1-A)/(1+A)| \leqslant 1$ always. Similarly, $|(1-B)/(1+B)| \leqslant 1$ and $|(1-E)/(1+E)| \leqslant 1$.

Hence, the scheme is unconditionally stable. The local truncation error is $O(\Delta t^2 + \Delta X^2 + \Delta Y^2)$ and it tends to zero as Δt, ΔX and ΔY tend to zero. Hence the scheme is compatible. Stability and compatibility ensures convergence.

5. Results and discussion

In order to get a physical insight into the problem, a representative set of numerical results is shown graphically in Figs. 1–9, to illustrate the influence of physical quantities such as radiation parameter N, Grashof number Gr, mass Grashof number Gm, Schmidt number Sc on velocity, temperature and concentration. All the computations are carried out for $Pr = 0.71$ (i.e., for air) and the corresponding values of Sc are chosen such that they represent helium (0.3), water vapor (0.6), ammonia (0.78), carbon dioxide (0.94) and ethyl benzene (2.0).

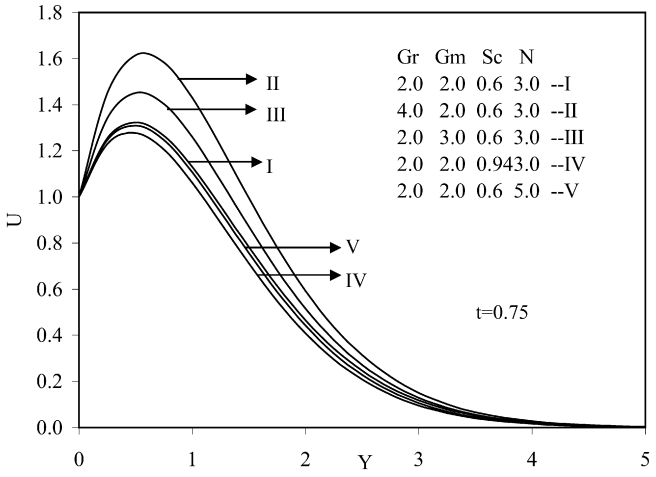

Fig. 1. Transient velocity profiles at $X = 1.0$ for different Gr, Gm, Sc, N.

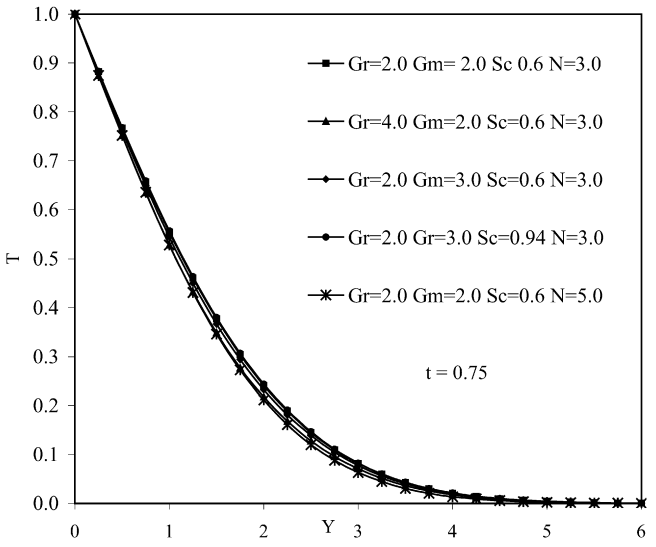

Fig. 2. Transient temperature profiles at $X = 1.0$ for different Gr, Gm, Sc, N.

Table 1
Time to reach steady-states

S. No	Gr	Gm	Sc	N	Steady-state values		
					Velocity	Temperature	Concentration
I	2	2	0.6	3	8.65	8.65	8.65
II	4	2	0.6	3	8.48	8.48	8.48
III	2	4	0.6	3	8.22	8.22	8.22
IV	2	2	2.0	3	7.58	7.58	7.58
V	2	2	0.6	5	9.54	9.54	9.54

The time taken to reach the steady-states of the velocity, temperature and concentration for different values of governing parameters is shown in Table 1. From Table 1, it is observed that the time taken for the velocity, temperature and concentration to reach the steady-state decreases with the increase in Gr or Gm or Sc, whereas it increases with the increase in radiation parameter N. The transient velocity, temperature and concen-

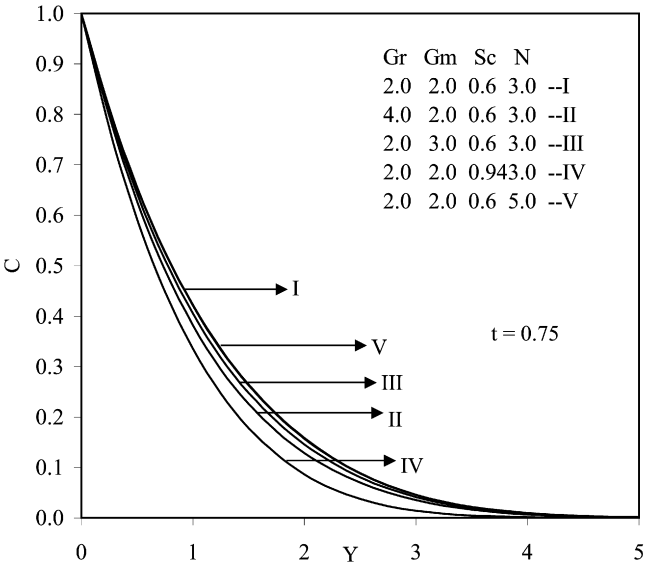

Fig. 3. Transient concentration profiles at $X = 1.0$ for different Gr, Gm, Sc, N.

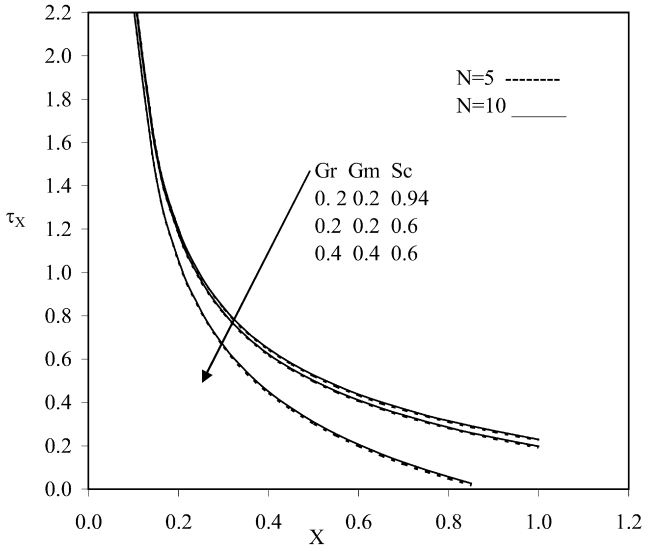

Fig. 4. Local skin-friction.

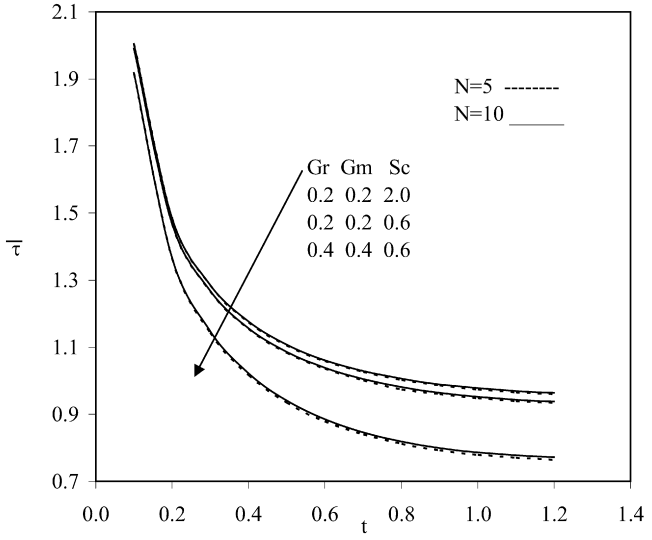

Fig. 5. Average skin-friction.

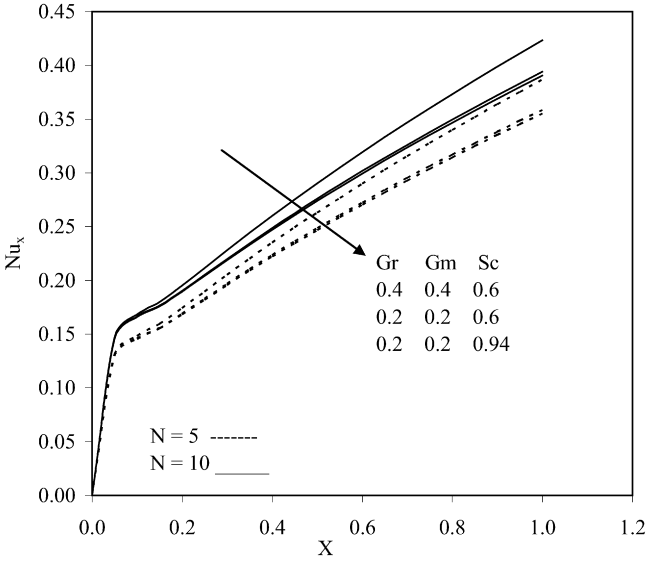

Fig. 6. Local Nusselt number.

tration profiles for different values of Gr, Gm, Sc and N at a particular time $t = 0.75$, are shown in Figs. 1–3. From Fig. 1, it is found that the transient velocity increases with the increase in Gr or Gm, whereas it decreases with the increase in Sc or N. It is noticed that the transient temperature decreases with the increase in N, whereas it increases with the increase in Sc (Fig. 2). It is interesting to note that, owing to an increase in the value of the radiation parameter N, both momentum and thermal boundary layer thickness decrease. From Fig. 3, it is seen that the transient concentration decreases with the increase in Gr or Gm or Sc, whereas it increases with the increase in N. It is also observed that increasing values of N corresponds to a thicker concentration boundary layer relative to the momentum boundary layer.

Steady-state local skin-friction τ_X profiles are plotted in Fig. 4 against the axial coordinate X. The local shear stress τ_X increases with the increasing value of Sc and decreasing value of Gr and Gm. The average values of skin-friction $\bar{\tau}$ for different Gr, Gm, Sc and N are shown in Fig. 5. It is noted that $\bar{\tau}$ decreases with decreasing values of Sc, but increases with decreasing values of Gr or Gm throughout the transient period and at the steady-state level. It is also observed that the average skin-friction $\bar{\tau}$ increases as the radiation interaction parameter N increases. The local Nusselt number Nu_X for different Gr, Gm, Sc and N are shown in Fig. 6. Local heat transfer rate Nu_X decreases with increasing values of Sc and increases with increasing Gr or Gm. For increasing values of radiation parameter N, the local Nusselt number Nu_X increases. The trend is just opposite in case of local Sherwood number Sh_X with respect to Gr, Gm, Sc and N (Fig. 7). From Fig. 8 it is observed that the average Nusselt number $\overline{Nu}$ increases with increasing values of Gr or Gm and N. From Fig. 9, we can easily see that the average Sherwood number $\overline{Sh}$ increases as Gr or Gm and Sc increases.

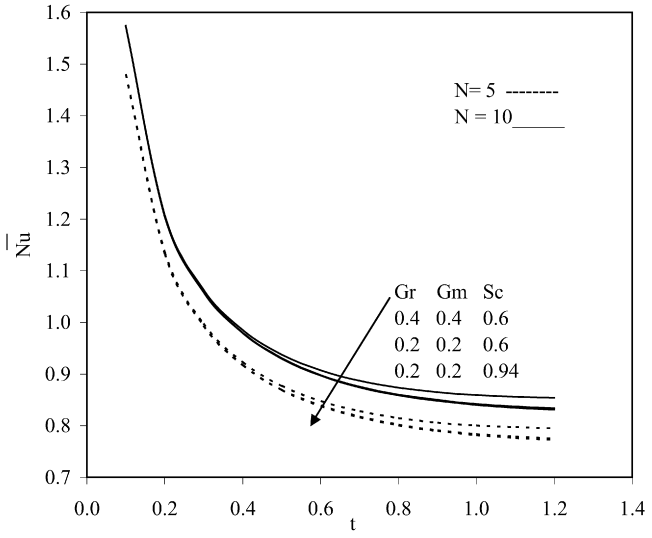

Fig. 7. Average Nusselt number.

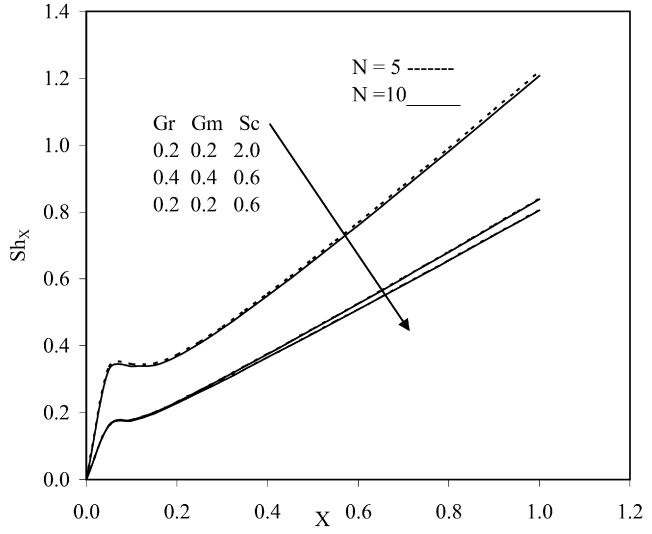

Fig. 8. Local Sherwood number.

6. Conclusions

A numerical study has been carried out to study the radiation effects past an impulsively started vertical plate in the presence of mass transfer. The fluid is gray, absorbing-emitting but non-scattering medium and the Rosseland approximation is used to describe the radiative heat flux in the energy equation. A family of governing partial differential equations is solved by an implicit finite difference scheme of Crank–Nicolson type, which is stable and convergent. The results are obtained for different values of radiation parameter N, thermal Grashof number Gr, solutal Grashof number Gm, and Schmidt number Sc. Conclusions of this study are as follows.

1. The time required for velocity to reach the steady-state increases as radiation parameter increases.
2. The momentum boundary layer thickness decreases with the increase Sc.

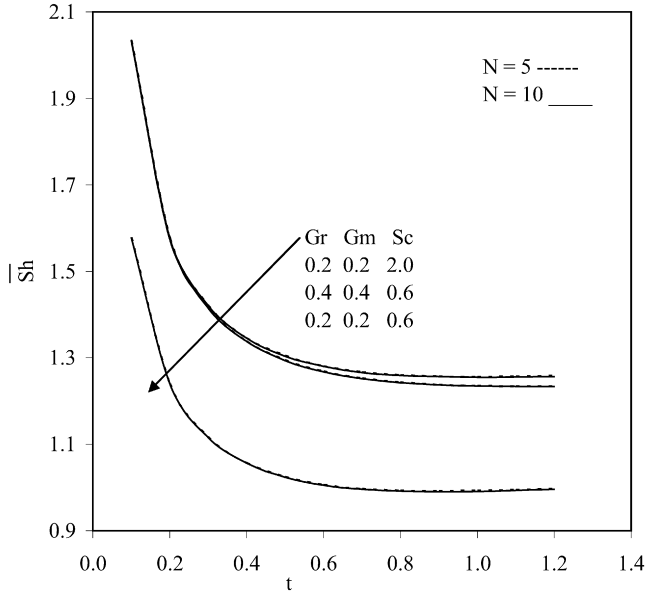

Fig. 9. Average Sherwood number.

3. At small values of the radiation parameter N, the velocity and temperature of fluid increases sharply near the plate as the time t increase, which is totally absent in the absence of radiation effects.
4. The local and average skin-friction decreases with the increasing Gr or Gm and increases with the increasing value of radiation parameter N and Schmidt number Sc.
5. The average Nusselt number increases with the increasing value of the radiation parameter N.
6. The average Sherwood number increases as Gr or Gm and Sc increases.

References

[1] G.G. Stokes, On the effect of internal friction of fluids on the motion of pendulums, Cambridge Phil. Trans. IX (1851) 8–106.

[2] K. Stewartson, On the impulsive motion of a flat plate in a viscous fluid, Quart. J. Mech. Appl. Math. 4 (1951) 182–198.

[3] M.G. Hall, Boundary layer over an impulsively started flat plate, Proc. Roy. Soc. London A 310 (1969) 401–414.

[4] V.M. Soundalgekar, Free convection effects on the Stokes problem for infinite vertical plate, ASME J. Heat Transfer 99 (1977) 499–501.

[5] A. Raptis, A.K. Singh, Free convection flow past an impulsively started vertical plate in a porous medium by finite difference method, Astrophys. Space Sci. 112 (1985) 259–265.

[6] V.M. Soundalgekar, Effects of mass transfer and free convection on the flow past an impulsively started vertical plate, ASME J. Appl. Mech. 46 (1979) 757–760.

[7] U.N. Das, R.K. Deka, V.M. Soundalgekar, Effects of mass transfer on flow past an impulsively started infinite vertical plate with constant heat flux and chemical reaction, Forschung im Ingenieurwesen – Engineering Research 60 (1994) 284–287.

[8] R. Muthucumaraswamy, P. Ganesan, Unsteady flow past an impulsively started vertical plate with heat and mass transfer, Heat Mass Transfer 34 (1998) 187–193.

[9] R. Muthucumaraswamy, P. Ganesan, First-order chemical reaction on flow past an impulsively started vertical plate with uniform heat and mass flux, Acta Mech. 147 (2001) 45–47.

[10] R. Muthucumaraswamy, P. Ganesan, Flow past an impulsively started vertical plate with variable temperature and mass flux, Heat Mass Transfer 34 (1999) 487–493.
[11] R.D. Cess, The interaction of thermal radiation with free convection heat transfer, Int. J. Heat Mass Transfer 9 (1966) 1269–1277.
[12] V.S. Arpaci, Effect of thermal radiation on the laminar free convection from a heated vertical plate, Int. J. Heat Mass Transfer 11 (1968) 871–881.
[13] E.H. Cheng, M.N. Ozisik, Radiation with free convection in an absorbing, emitting and scattering medium, Int. J. Heat Mass Transfer 15 (1972) 1243–1252.
[14] A. Raptis, Radiation and free convection flow through a porous medium, Int. Comm. Heat Mass Transfer 25 (1998) 289–295.
[15] M.A. Hossain, H.S. Takhar, Radiation effect on mixed convection along a vertical plate with uniform surface temperature, Heat Mass Transfer 31 (1996) 243–248.
[16] M.H. Mansour, Radiative and free convection effects on the oscillatory flow past a vertical plate, Astrophys. Space Sci. 166 (1990) 26–75.
[17] A. Raptis, C. Perdikis, Radiation and free convection flow past a moving plate, Appl. Mech. Eng. 4 (1999) 817–821.
[18] U.N. Das, R.K. Deka, V.M. Soundalgekar, Radiation effects on flow past an impulsively started vertical plate – an exact solutions, J. Theor. Appl. Fluid Mech. 1 (1996) 111–115.
[19] A.J. Chamkha, H.S. Takhar, V.M. Soundalgekar, Radiation effects on free convection flow past a semi-infinite vertical plate with mass transfer, Chem. Engrg. J. 84 (2001) 335–342.
[20] M.Q. Brewster, Thermal Radiative Transfer and Properties, John Wiley & Sons, New York, 1992.
[21] B. Carnahan, H.A. Luther, J.O. Wilkes, Applied Numerical Methods, John Wiley & Sons, New York, 1969.